Adsorption properties of graphene oxide/chitosan microspheres for removal of Cr (VI) from aqueous solutions

Zhengyuan Song[a], Tao Feng[a,b],*, Yimin Hu[a], Li Wang[a], Xiaoqing Zhang[a]

[a]*College of Resources and Environmental Engineering, Wuhan University of Science and Technology, Wuhan 430081 China, Tel. +86 27 68862880, email: 2430502028@qq.com (Z. Song), hymwust@163.com (Y. Hu), Tel. +86 27 68862885, emails: wanglijohn@163.com (L. Wang), 396610331@qq.com (X. Zhang)*
[b]*Hubei Key Laboratory for Efficient Utilization and Agglomeration of Metallurgic Mineral Resources. Wuhan University of Science and Technology, Wuhan 430081 China, Tel. +86 27 68862880, email: fengtaowhu@163.com (T. Feng)*

ABSTRACT

The graphene oxide (GO) and graphene oxide/chitosan micro spheres (GOCS) for removal of hexavalent chromium were prepared and characterized by fourier transform infrared spectroscopy (FT-IR), X-ray diffraction (XRD), scanning electron microscope (SEM) and transmission electron microscope (TEM). The adsorption behavior of the GOCS and chitosan (CS) micro spheres for Cr (VI) was studied, and the effects of solution pH, adsorption time, and initial metal ion concentration on adsorption capacity of the adsorbent were also investigated. The adsorption capacities of GOCS and CS were found to be 197.6 mg/g and 129.9 mg/g, respectively. The characteristics of the adsorption process were evaluated by using the Langmuir and Freundlich isotherm models. The adsorption processes fit better with the Langmuir model. The adsorption of Cr (VI) on GOCS was a typical mono molecular layer adsorption. The pseudo-first-order and pseudo-second-order kinetic models were employed to describe the kinetic processes, and the results indicated that the adsorption of Cr (VI) followed a second-order type reaction kinetics.

Key words: Graphene oxide; Chitosan; Microsphere; Adsorption; Hexavalent chromium

1. Introduction

Chromium is widely used in metallurgical, electroplating, production of paints, pigments, tanning, and wood preservation [1–3]. Chromium mainly exists in two states namely Cr (III) and Cr (VI) in environment [4]. Cr (VI) not only performs great toxicity, which is 500 times to Cr (III), but also has severe carcinogenicity and mutagenicity [5]. In addition, Cr (VI) has strong oxidability and mobility. The effluents with chromium dumped into the natural waters leading a serious threat to ecological environment, as well as human health [6,7].

Various methods of removing Cr (VI) from effluents have been investigated, such as chemical precipitation [8], reverse osmosis [9,10], adsorption, and ion exchange [11].

Among these methods, adsorption is a popular method because of its prominent advantages, such as high efficiency, low cost, ease of operation and so on. In this method, the key is to choose an appropriate absorbent. An excellent absorbent must have large specific surface area, chemical stability, and a large number of adsorption sites [12].

Being one of the important graphene derivatives, graphene oxide (GO) has good affinity and solubility in water and easy to be chemical modified as its oxygen functional groups existing in the surface. [13,14]. Moreover, the surface area of GO is large. Due to these advantages, GO is widely used in water treatment. However, GO is difficult to be separated from aqueous solutions. And there are many acidic functional groups on the surface, which is the reason why GO performs electronegative in water. So, many researchers grafted the amino groups or other alkaline groups on the surface of GO, and study the adsorption properties of removing Cr(VI) and other negative ions in

*Corresponding author.

water [15,16]. Chitosan (CS), as a natural electro positive alkyl polysaccharide polymer without toxic effect, is one of environment-friendly and low-cost biosorbents [17]. Chitosan has great ability to adsorb different ions as a result of having a quantity of the hydroxyl and amino groups [18], especially many heavy metal ions and dyes that are difficult to be removed. Therefore, the research on the adsorption properties of graphene oxide/chitosan composites has become a popular direction.

In this study, graphene oxide (GO) and graphene oxide/chitosan micro spheres (GOCS) for removal of hexavalent chromium were prepared. The adsorbents were characterized by Fourier transform infrared spectroscopy (FTIR), X-ray diffraction (XRD), scanning electron microscope (SEM) and transmission electron microscope (TEM). The adsorption capacity of GOCS on the removal of Cr(VI) was studied using batch studies. The effects of pH, initial concentration, contact time, and dosage on the adsorption were investigated in detail. The adsorption kinetics and isotherms for Cr(VI) onto GOCS were also analyzed.

2. Materials and methods

2.1. Materials

Natural Flake graphite powder, with 325 mesh, was purchased from Jinrilai graphite co. Ltd in Qingdao. Chitosan (CS) with a degree of deacetylation more than 90% was obtained from Zhejiang Ocean Biochemical Company. $NaNO_3$, $KMnO_4$, H_2O_2, $K_2Cr_2O_7$, ethanol, NaOH, HCl, Span-80, liquid paraffin, glacial acetic acid, formaldehyde and epichlorohydrin (ECH) were also of analytical grade. The water used in the experiments was ultra pure water.

2.2. Preparation of GO

GO was prepared from natural flake graphite by the modified Hummers method [19]. 75 ml 98% H_2SO_4 was added to the 500 mL three flasks with 3.0 g of natural flake graphite powder and 0.75 g of $NaNO_3$. Stirring slowly with electric mixer for 30 min, and keep the temperature at about 4°C by putting the three flasks in ice bath. Then 9.0 g $KMnO_4$ was added into the tree flasks in batches, and stirred vigorously for 3 h. Until the solution turned to purple green, move the device to water bath which was maintained about 35°C, and stirred for 1 h. 140 mL of ultra pure water was added to tree flasks with vigorous stirring, while retaining the reaction temperature at 98°C. After hydrolyzed for 40 min, added appropriate amount of H_2O_2 into the mixer whose color changed to a bright yellow, and kept stirring until there were no bubbles. Filter the production from the mixture when it was still hot. The production was washed to neutral with 5% HCl, ultra pure water and ethanol and dried under 60°C in vacuum oven for 24 h. The GO was obtained after grinded and sifted.

2.3. Preparation of GOCS and CS micro spheres

Certain amount of prepared GO was dispersed into 100 ml 2% (v/v) acetic acid solution. Various concentration of GO suspension was obtained after ultrasonicated

for 30 min. 4.0 g chitosan was added into GO suspension and stirred for 3 h. 120 ml liquid paraffin and a small amount of span-80 were added to the graphene oxide/chitosan mixture, while stirred vigorously for 1 h. Then added 37.5 ml 40% formaldehyde for pre-cross linking, and kept stirring for about 2 h. Followed on pouring the mixture into a large amount of solution, in which the volume ratio of absolute ethanol and 10% NaOH was 1:1, and stirred slowly for another 3 h. The pre-cross linked GOCS micro spheres had been obtained after filtrated and washed. Next, put the micro spheres into 350 ml 0.06 mol/L NaOH solution, added appropriate amount of ECH, stirred slowly under 70°C for 3 h. The micro spheres were immersed in 5% HCl for a whole night after filtrated. Then after washed and filtrated again, immersed the micro spheres in 5% NaOH for several hours. Finally, the production was dried in vacuum at 60°C after washed several times by distilled water until the pH was close to 7. The CS micro spheres were prepared under the same conditions without the addition of GO suspension and used as controls.

2.4. Characterization

Grinded the micro spheres into powder, then mixed the samples and KBr at the ratio of 1:100 (w/w). FTIR spectra were recorded with KBr pellets on Nicolet-360 FT-IR spectrometer. The images of materials were recorded with a Nava 400 Nano scanning electron microscope (SEM) (Philips, FEI Co., America) and a transmission electron microscope (TEM)(Hitachi, H-9500, Japan). X-ray diffraction (XRD) measurement was conducted on a Rigaku D/max-IIIA X-ray diffractometer using Cu Kα radiation (λ = 0.1544 nm).

2.5. Batch experiments

The batch experiments adopted the method of static adsorption. Measured 50 ml Cr (VI) solution of certain concentration into conical flask. 50 mg prepared CS and GOCS micro spheres were added into the solution respectively after adjusted the pH by using NaOH and HCl. Put the conical flask on double multi-purpose speed oscillator with 200 rpm for desired time under room temperature. The concentration of Cr (VI) was detected by flam atomic absorption spectrophotometry (FAAS).

The removal rate (R) was calculated from Eq. (1).

$$R = \frac{(C_0 - C_e)}{C_e} \times 100\% \tag{1}$$

The adsorption capacity (Q) of micro spheres was calculated from Eq. (2).

$$Q = \frac{(C_0 - C_e)V}{1000m} \tag{2}$$

where C_0, C_e represent the concentration (mg/L) of Cr (VI) before and after adsorption, respectively. V (L) is the volume (50 mL) of the solution, m (g) is the mass of the dry adsorbent.

3. Results and discussion

3.1. Characterization of the materials

3.1.1. Morphology of materials

Fig. 1 shows the transmission electron microscope images of GO with different ultrasonic time. As can be seen in Fig. 1a, the edges of GO have folds, which may be appeared in the preparation for graphene oxide production process, showing the state of superposition. This may be due to the short of ultrasonic time and incomplete exfoliation. According to Fig. 1b, there are still some of the GO multilayer overlay when the ultrasonic time is 15 min. But compared with Fig. 1a, the stacked layer is evidently decreased. From Figs. 1c and d, the GO appears to be lamellar structure, the stack layers are less than the formers. As well as the surface become smoother and thinner. The multi-layer structure of GO indicated that the Van der Waals' force between the layer is large. And with the increase of the ultrasonic time, the better peel effect is.

Fig. 2 is the SEM images of CS micro spheres and GOCS micro spheres. As seen in the images, the CS micro spheres (a) are spherical in shape and the particles are micron-size, which is about 500 μm. The surface of the particles appears to be
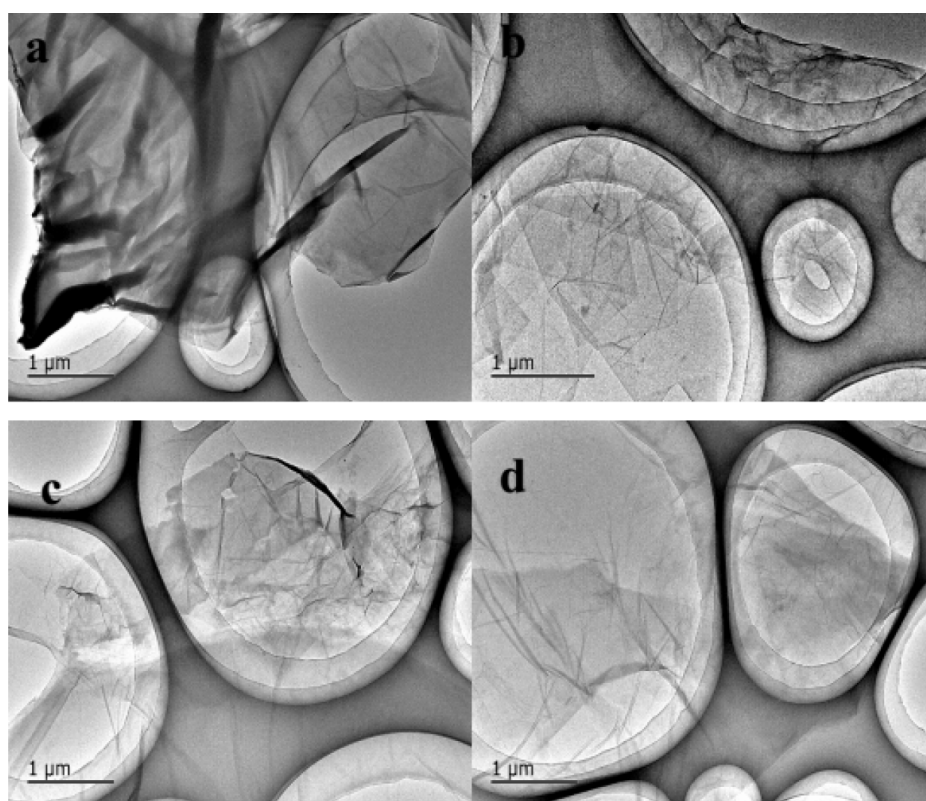
Fig. 1. TEM image of GO with different ultrasonic time (a: 5 min, b: 15 min, c: 30 min, d: 60 min).
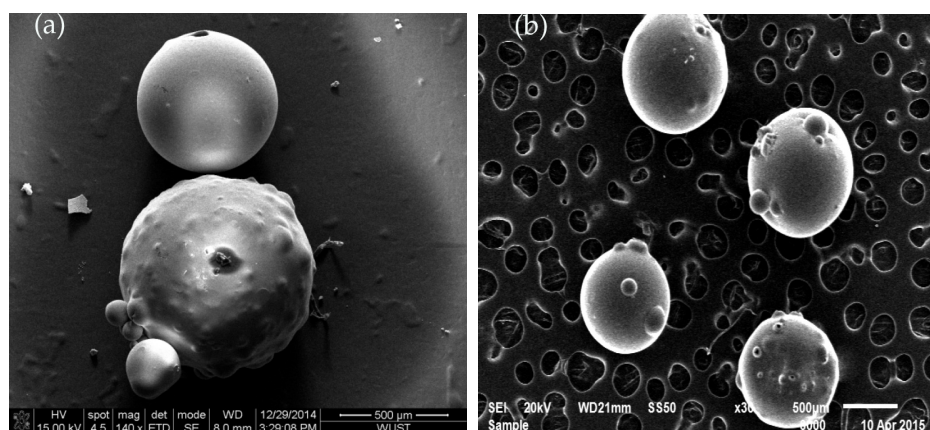
Fig. 2. SEM images of CS micro spheres(a) and GOCS micro spheres(b).

smooth. The morphology of GOCS micro spheres (b) is similar to that of CS micro spheres. GOCS micro spheres are spherical in shape with small spherule on the surface and the size is about 500 μm. The SEM results showed that the morphology of GOCS is more uniform and have good mono dispersity.

3.1.2. XRD analysis

The XRD patterns of graphite (a) and GO (b) are shown in Fig. 3. As shown, the XRD patterns of graphite and GO are different apparently. Graphite has a regular layered structure, a strong diffraction peak appears at $2\theta = 26.5°$. According to the Bragg equation $2d \sin\theta = \lambda$, the layer spacing can be calculated to be 0.34 nm. Compared with graphite, the peak of GO at $2\theta = 26.5°$ has been disappeared totally. Instead, a new diffraction peak appears at $2\theta = 10.7°$. The layer spacing can be calculated to be 0.82 nm, which is in accordance with the previous report [20]. The change indicated that the graphite had been completely converted to GO after a series of oxidation reaction and ultrasonic treatment. According to Wilson's study [21], the reason why layer spacing of GO is bigger than that of graphite is the graphite sheet formed polar oxygen group in the process of strong oxidation, and the hydrophilicity of the graphite oxide layer was enhanced so that the water molecules were inserted into the graphite oxide layer. The bigger layer spacing is benefit to the intercalation of small molecules and polymers.

3.1.2. FTIR analysis

Fig. 4 shows the FTIR spectra of GO, GOCS and CS. As shown in Fig.4a, the predominant peaks at 1740 and 3444 cm^{-1} correspond to C=O stretching vibrations of the –COOH groups and O–H stretching vibration, respectively. (The peaks at 1645 cm^{-1} correspond to C–C stretching mode of the sp^2 carbon skeletal network) [22]. The FTIR spectra of CS is shown in Fig. 4c, which is similar with what the literature recorded [23]. The broad adsorption peak at 3439 cm^{-1} is the multiple absorption peaks overlapped by stretching vibration of –NH$_2$, N-H and O-H in chitosan. The peak

around 1072 cm^{-1} is the adsorption peak of C$_3$-OH at C$_3$ of chitosan. The peak of amide band appeared at 1643 cm^{-1}. Fig. 4b is the FTIR spectra of GOCS components. As can be seen from the graph, there are similarities among GOCS, CS and GO, but slightly different. The peak at 3438 cm^{-1} is the adsorption peak overlapped by –NH$_2$, N-H, O-H in CS and O-H in GO. The peak at 1645 cm^{-1} is the stretching vibration of C=C in GO. The intensity of these peaks were significantly blue shift than that of GO, due to the existence of hydrogen bonds between CS and GO.

3.2. Factors that affect the Cr (VI) adsorption

3.2.1 Effect of GO concentration on adsorption capacity

4.0 g chitosan was added into a series of 100 mL graphene oxide suspension, which concentration is 0, 0.25 g/L, 0.5 g/L, 1.0 g/L, 2.0 g/L, 3.0 g/L, respectively, to prepare the GOCS micro spheres. So that the mass ratio of GO and CS was 0, 0.025:4, 0.05:4, 0.1:4, 0.1:2, 0.3:4, respectively. Adsorption experiments were conducted by adding 0.05 g of GOCS micro spheres into 50 mL Cr (VI) solutions whose pH was adjusted to about 5 in conical flasks and shake for 180 min at 200 rpm.

As shown in Fig. 5, the adsorption capacity of CS micro spheres was 71.41 mg/g. With the addition of GO, the adsorption capacity of GOCS micro spheres was significantly higher than that of CS micro spheres. When the GO concentration reached 1.0 g/L (the mass ratio of GO and CS was 0.1:4), the adsorption capacity was 90.68 mg/g. With further increasing the GO concentration, the adsorption capacity of GOCS was decreased gradually. Chitosan intercalated into graphene oxide along with the addition of GO, the combination of two substances presented new properties, such as the increase of the surface area, which result in the adsorption capacity increasing. While the GO concentration increased beyond 1.0 g/L, the content of CS on GOCS micro spheres is decreased relatively. The reduction of amino led to the decrease of adsorption capacity, since the amino groups on CS play an important role in adsorbing.
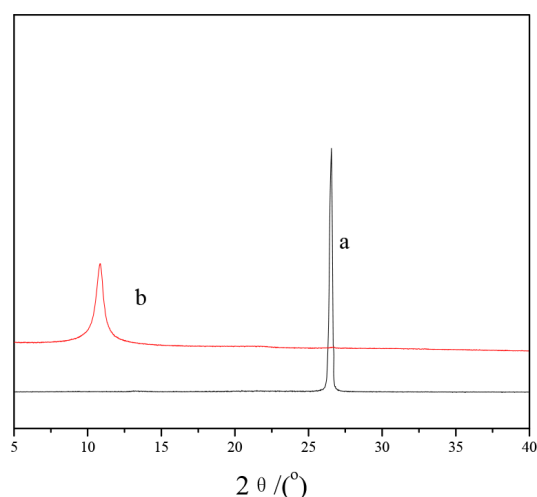
Fig. 3. XRD patterns of graphite (a) and GO (b).
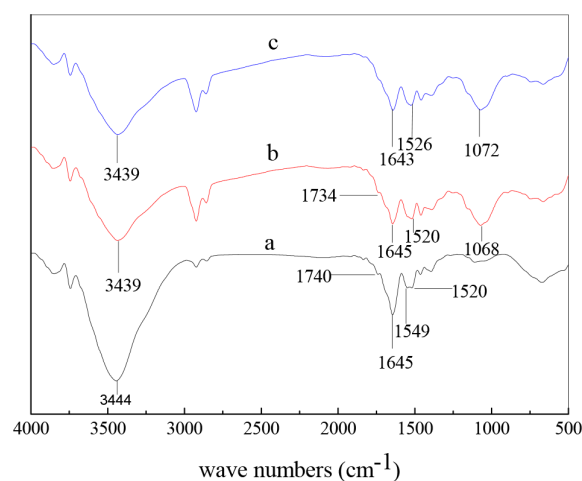
Fig. 4. FTIR spectra of GO (a), GOCS micro spheres (b) and CS micro spheres (c).

Fig. 5. Effect of GO concentration on adsorption capacity.
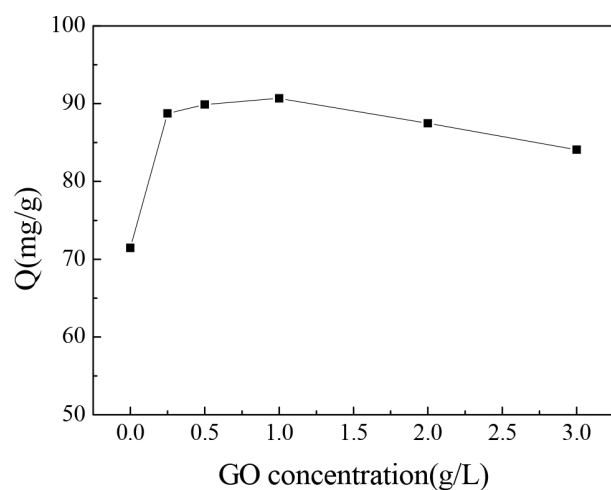
Fig. 6. The effect of pH on adsorption capacity.

3.2.2. Effect of pH on adsorption capacity

The pH is the most important factor affecting the adsorption process. Since the radius of hydrolyzed cation and the charge of the adsorbent surface will be changed along with the change of pH. To investigate the effect of pH on the adsorption performance, the initial pH values was adjusted from 2.0 to 5.0 by 0.1 mol L^{-1} HCl or 0.1 mol L^{-1} NaOH solutions. As Fig. 6 shows, when the pH was between 2.0 and 3.0, the adsorption capacities of two materials were increased with pH increasing. But when the pH was between 3.0 and 5.0, the tendencies of two materials were different. The adsorption capacity of GOCS was tending towards stability with pH increasing. It reached the maximum value (88.53 mg/g) at pH 5.0. While the adsorption capacity of CS was decreased with pH increasing. The surface charge of the adsorbent was strongly affected by the pH of the aqueous solutions [24] The $-NH_2$ of chitosan can be combined with H^+, and exist the following balance:

$$H^+ + RNH_2 \leftrightharpoons RNH_3^+$$
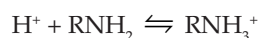
This behavior will enhance the electrostatic attraction of anions, and increasing the adsorption capacity of Cr(VI), which exists in anionic forms including $Cr_2O_7^{2-}$, $HCrO_4^-$, CrO_4^{2-}, and $HCr_2O_7^-$ in aqueous medium, and the fraction is depend on chromium concentration and pH [25]. With the increase of pH, H^+ in the solution was decreased. According to the equilibrium, the formation of RNH_3^+ from amino in chitosan by protonation was inhibited. This may weaken the electrostatic attraction of chitosan micro spheres, and more and more hydroxyl ions competed with the target ions, which caused the decrease in the adsorption capacity. It is obvious that GOCS performed a better adsorption property in a wide range of pH.

3.2.3. Effect of contact time on adsorption capacity

Contact time studies are helpful in understanding the amount of target ions adsorbed at various time by a fixed
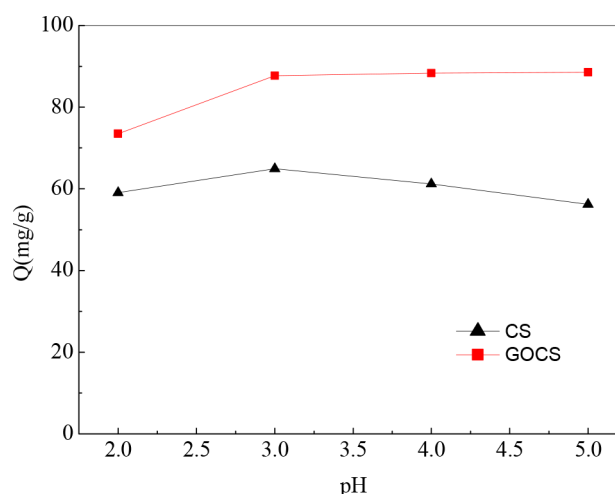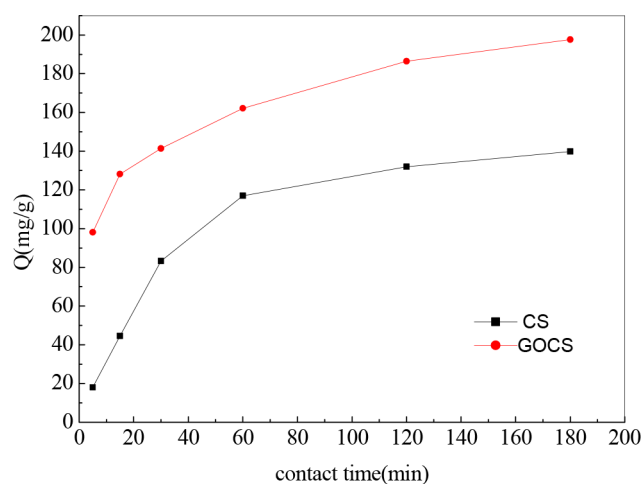
Fig. 7. The effect of contact time on adsorption capacity.

amount of the adsorbent. To investigate the effect of contact time on adsorption of Cr (VI), 0.05 g adsorbent and 50 mL Cr (VI) solution (initial concentration 400 mg L^{-1}) were used and the results are shown in Fig. 7.

As shown, it distinctly indicates that the adsorption of GOCS was a rapid process in the first 15 min, then followed by a slow process until attained equilibrium. But for CS micro spheres, the rapid adsorption process was at first 60 min, then followed by a slow adsorption process. At the initial stage of adsorption, a large number of vacant surface sites are available, the target ions are easy to combine with adsorption sites. As contact time goes on, the concentration of Cr (VI) is decreased, and the remaining vacant surface sites are difficult to be occupied due to repulsive forces between Cr (VI) adsorbed on the surface of adsorbents and solution phase. As a consequence, the adsorption rate slowed down, and achieved the dynamic equilibrium finally. Under our experimental conditions, the maximal adsorption capacity of CS and GOCS microspheres were 127.3 mg g^{-1} and 192.8 mg g^{-1}, respectively.

3.2.4. *Effect of initial concentration on adsorption capacity*

The effect of the initial Cr(VI) concentration on adsorption capacity was carried out by vibrating 100 mL various concentrations of Cr(VI) solution (100 mg/L, 200 mg/L, 300 mg/L, 400 mg/L and 500 mg/L) with 0.1 g adsorbent at room temperature for 180 min. As shown in Fig. 8, when the initial concentration of Cr(VI) increased from 100 to 500 mg L^{-1}, the adsorption capacity of CS and GOCS increased from 67.92 to 129.94 mg g^{-1} and 88.53 to 197.62 mg g^{-1}, respectively. It can be seen that an increase in the initial Cr (VI) concentration leads to an increase in mass gradient between the solution and adsorbent, and thus acts as a driving force for overcoming the transfer resistance between the adsorption medium and adsorbent [26]. With increasing of the initial concentration, more active sites of CS and GOCS involve in the adsorption process. Higher ions concentration not only enhanced the mass transfer driving force, but also increased the number of collisions between metal ions and the adsorbent. Therefore, the ions uptake capacity in equilibrium is certainly increased [27,28].

3.3. *Adsorption isotherm*

Adsorption isotherm is a critical factor to assess whether the adsorbents are effective and feasible. The relationship between the Cr(VI) ions adsorbed by the adsorbent surface and the remaining Cr(VI) ions concentration in the aqueous phase at equilibrium can be observed by adsorption isotherm models. Two isotherm models, Langmuir and Freundlich model, were applied to simulate the experimental data. Langmuir isothermal adsorption model assumes that the adsorption is monolayer adsorption. When a site is occupied by an adsorbate molecule, there is no more adsorption take place at this site [29].

The equation of the Langmuir adsorption model is shown in Eq. (3).

$$Q_e = \frac{Q_0 b C_e}{1 + b C_e} \tag{3}$$

The linear equation of Eq. (3) was as follows:

$$\frac{C_e}{Q_e} = \frac{C_e}{Q_0} + \frac{1}{Q_0 b} \tag{4}$$

Langmuir adsorption constant R_L (L mg^{-1}) is an important parameter to measure whether the adsorption system is effective or not, which is related to the affinity of binding sites. The value of the parameter R_L indicates the type of isotherm is unfavorable ($R_L > 1$), linear ($R_L = 1$), favorable ($0 < R_L < 1$), or irreversible ($R_L = 0$) [30]. The formula is as Eq. (5).

$$R_L = \frac{1}{1 + b C_0} \tag{5}$$

where the Q_e (mg/g) represents the equilibrium adsorption capacity and Q_0 (mg/g) is the maximum adsorption capacity of Cr (VI). C_e (mg/L) is the equilibrium concentration of Cr (VI) in aqueous solution. b (g/mg) is the Langmuir constant related to the affinity of the binding sites. C_0 (mg/L) is the initial concentration of Cr (VI) in aqueous solution.

Freundlich isothermal adsorption model assumes that the adsorption is multi molecular layer adsorption, which is purely empirical. Because the existing form of adsorption sites and the adsorbed metal ions in the solution are various.

The equation of the Freundlich adsorption model is shown in Eq. (6).

$$Q_e = k C_e^{\frac{1}{n}} + C \tag{6}$$

In order to calculating and fitting, Eq. (6) has a deformation equation as Eq. (7).

$$\ln Q_e = \ln k + \left(\frac{1}{n}\right) \ln C_e \tag{7}$$

where k is the Freundlich constant that is related to the adsorption capacity, $1/n$ is the Freundlich constant that is related to the adsorption intensity, C is the constant.

The calculated results are shown in Table 1, and the fitted curve is shown in Fig. 9.

Fig. 8. The effect of initial concentration on adsorption capacity..
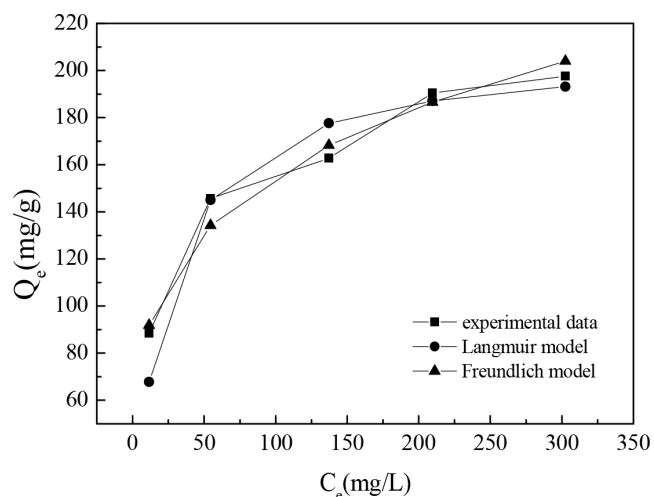
Fig. 9. Adsorption isotherms of GOCS micro spheres.

As shown in Table 1, the correlation coefficient R^2 of Langmuir adsorption model and Freundlich adsorption model of GOCS micro spheres is 0.9937 and 0.975, respectively. The correlation coefficient R^2 of Langmuir model, which is more than 0.99, is higher than that of Freundlich model. It was obvious that the Langmuir model fitted better than Freundlich model on adsorption of Cr (VI) on GOCS. The theoretical maximum adsorption capacity of GOCS micro spheres calculated by Langmuir equation is 208.3 mg/g, and the experimental data (197.6 mg/g) is almost reach the theoretical maximum adsorption capacity. It may be attributed to the incomplete contact of Cr (VI) and the adsorbent [30]. Thus, it can be proposed that the sorption behavior of Cr (VI) onto GOCS is considered to be representative of sorption onto a monolayer. Moreover, the adsorption sites on the GOCS may be finite and homogeneously distributed over the adsorbent surface. The R_L can be calculated by Eq. (5), and the result is shown to be in the ranges 0.045~0.192. According to the reference [4], when the R_L value is between 0 and 1, the adsorption process is considered to be favorable.

3.4. Kinetic studies

In order to investigate the adsorption kinetics of Cr(VI) in aqueous solution by GOCS, the pseudo-first-order and pseudo-second-order rate models were used for testing the dynamic experimental data.

The pseudo-first-order rate expression of Lagergren [31] is as Eq. (8).

$$\frac{dQ_t}{dt} = k_1 t \left(Q_e - Q_t\right) \tag{8}$$

The rearranged form of Eq. (8) is

$$\ln\left(Q_e - Q_t\right) = \ln Q_e - k_1 t / 2.303 \tag{9}$$

The pseudo-second-order rate model is as Eq. (10).

$$\frac{t}{Q_t} = \frac{1}{k_2 Q_e^2} + \frac{1}{Q_e} t \tag{10}$$

where Q_e is on behalf of equilibrium adsorption capacity (mg g^{-1}) of adsorbent, Q_t is representative of adsorption capacity (mg g^{-1}) of adsorbent when time is t. k_1 and k_2 are the constant (g (mg·min)$^{-1}$) of first-order rate model and second-order rate model, respectively.

According to the data in Fig. 7 and the equation mentioned above, the fitting results are shown in Table 2. As seen in Table 2, the correlation coefficient of second-order rate model of two materials is 0.9921 and 0.9965. The correlation coefficient of first-order rate model of two materials is 0.9767 and 0.9933, respectively. But the theoretical equilibrium adsorption capacity of CS and GOCS are 151.5 mg/g and 204.1 mg/g, calculated by pseudo-second-order model, which are close to the experimental data. Although two types of kinetic model are all fit well with the adsorption process, the pseudo-second-order model is a better descriptor of the adsorption process, indicating a chemisorption process. The rate constant of second-order adsorption model of CS is 0.22×10^{-3} g (mg·min)$^{-1}$, which is lower than that of GOCS (0.47×10^{-3} g (mg·min)$^{-1}$). It can be concluded that the initial rate of adsorption on GOCS is faster than that of CS.

3.5. The regenerative adsorption property of GOCS

For practical application, recycling and regeneration of the adsorbent is indispensable. It can not only recover the metal resource removed from the wastewater, but also lead to reusability of the adsorbent. The regeneration ability of an adsorbent makes the adsorption process more economic and applicable [32]. 0.5 mol/L NaOH and 0.1 mol/L HCl were used to treat GOCS which has adsorbed Cr (VI) for the removal of the adsorbed ions. Fig. 10 shows the adsorption capacity of GOCS and the removal efficiency of Cr (VI) after using the same GOCS for five times. It is shown that the adsorption capacity of Cr (VI) on the adsorbents decreased slowly with increasing cycle number. The initial adsorption capacity of GOCS was 88.53 mg/g. After regeneration and reused for five times, the adsorption capacity of GOCS was 85.74 mg/g, 80.21 mg/g, 75.42 mg/g and 68.25 mg/g, respectively. It is found that the adsorption capacity remains 77.1% of initial value at fifth cycle. The slight adsorption

Table 1
Adsorption isotherm parameters of GOCS microspheres and CS microspheres

Adsorption	Freundlich adsorption model			Langmuir adsorption model			
Materials	n	K	R^2	q	B	R^2	R_L
CS	3.652	26.48	0.9936	144.9	0.021	0.9953	0.087~0.322
GOCS	4.101	50.66	0.975	208.3	0.042	0.9937	0.045~0.192

Table 2
The fitting conditions of adsorption of Cr(VI) on GOCS and CS

Adsorbents	Adsorption capacity	First-order kinetics			Second-order kinetics		
	$q_{e(exp)}$ (mg/g)	K_1	$q_{e(cal)}$ (mg/g)	R^2	K_2	$q_{e(cal)}$ (mg/g)	R^2
CS	144.9	0.0412	115.5	0.9767	0.22×10^{-3}	151.5	0.9921
GOCS	208.3	0.0502	103.1	0.9933	0.47×10^{-3}	204.1	0.9965
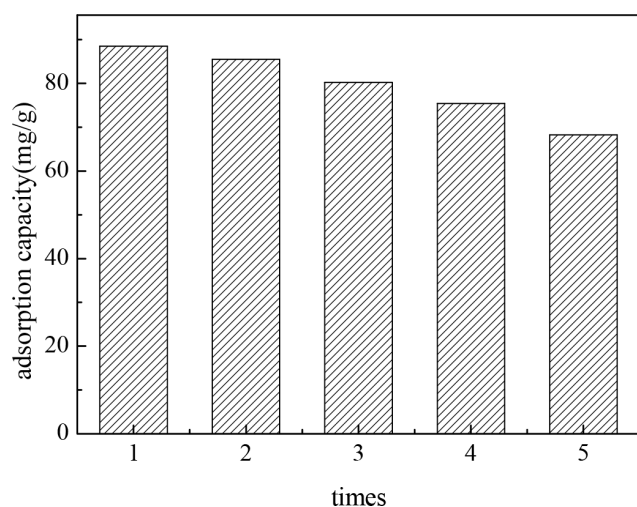
Fig. 10. The histogram of reusing of GOCS micro spheres.

capacity decrease may be due to the Cr (VI) adsorbed on GOCS cannot be completely desorbed and the active sites of GOCS were decreased. In summary, GOCS prepared in this work can be used repeatedly as an advanced adsorbent for practical treatment of Cr(VI) in wastewater.

4. Conclusions

The GO and GOCS micro spheres for removal of hexavalent chromium were successfully prepared and characterized by FT-IR, XRD, SEM and TEM. The GOCS micro spheres had a laudable performance for Cr (VI) adsorption. The maximum adsorption capacity of Cr (VI) was 208.3 mg g^{-1} based on Langmuir isotherm model. The results demonstrate that the adsorption process is dependent on pH, initial solution concentration, contract time and adsorbent dosage. .Langmuir isotherm was the most suitable adsorption isotherm for Cr(VI) sorption, and pseudo-second-order kinetic model was the most suitable kinetic model for the adsorption of Cr(VI) on GOCS micro spheres.

5. Contract grant sponsor

References

[1]   I. Marzouk, C. Hannachi, L. Dammak, B. Hamrouni, Removal of chromium by adsorption on activated alumina, Desal. Water Treat., 26 (2011) 279–286
[2]   S.M. Ponder, J.G. Darab, T.E. Mallouk, Remediation of Cr (VI) and Pb (II) aqueous solutions using supported, nano scale zero-valent iron, Environ Sci. Technol., 34 (2000) 2564–2569.
[3]   S.S. Chen, C.Y. Cheng, C.W. Li, P.H. Chai, Y.M. Chang, Reduction of chromate from electroplating wastewater from pH 1 to 2 using fluidized zero valent iron process, J. Hazard Mater., 142 (2007) 362.
[4]   A Kara, Adsorption of Cr (VI) ions onto poly (ethylene glycol dimethacrylate-1-vinyl-1,2,4-triazole), J. Appl Polym Sci., 114 (2010) 948–955.
[5]   L. Tang, G.D. Yang, G.M. Zeng, Y. Cai, S.S. Li, Synergistic effect of iron doped ordered mesoporous carbon on adsorption-coupled reduction of hexavalent chromium and the relative mechanism study, Chem Eng J., 239 (2014) 114–122.
[6]   R. Zhang, H Yi, Enhanced Cr^{6+} biosorption from aqueous solutions using genetically engineered Saccharomyces cerevisiae, Desal. Water Treat., 72 (2017) 290–299.
[7]   C. Namasivayam, M.V. Sureshkumar, Removal of chromium(VI) from water and wastewater using surfactant modified coconut coir pith as a biosorbent, Bioresour Technol., 99 (2008) 2218–2225.
[8]   S. Hanif, A. Shahzad, Removal of chromium (VI) and dye Alizarin Red S (ARS) using polymer-coated iron oxide (Fe_3O_4) magnetic nanoparticles by co-precipitation method, J. Nanopart. Res., 16 (2014) 2429.
[9]   A. Hafez, S. El-Mariharawy, Design and performance of the two-stage/two-pass RO membrane system for chromium removal from tannery wastewater, Desalination., 165 (2004) 141–151.
[10] A. Cimen, Removal of chromium from wastewater by reverse osmosis, Russ. J. Phys. Chem. A., 89 (2015) 1238–1243.
[11] M.S.M. Eldin, A.S. Al-Bogami, K.M. Aly, Z.A. Khan, A.E.M. Mekky, T.S. Saleh, A.A.W. Hakamy, Removal of chromium(VI) metal ions using Amberlite IRA-420 anions exchanger, Desal. Water Treat., 60 (2017) 335–342.
[12] J. Zhao, W. Ren, H.M. Cheng, Graphene sponge for efficient and repeatable adsorption and desorption of water contaminations, J. Mater Chem., 22 (2012) 20197–20202.
[13] A.K. Geim, K.S. Novoselov, The rise of graphene, Nat. Mater., 6 (2007) 183.
[14] D. Pandey, R. Reifenberger, R. Piner, Scanning probe microscopy study of exfoliated oxidized graphene sheets, Surf. Sci., 602 (2015) 1607–1613.
[15] H. Sojoudi, J. Baltazar, L.M. Tolbert, C.L. Henderson, S. Graham, Creating graphene p–n junctions using self assembled monolayers, ACS Appl. Mater. Inter., 4 (2012) 4781.
[16] J. Ou, Y. Wang, J. Wang, S. Liu, Z. Li, Self-assembly of octadecyltrichlorosilane on graphene oxide and the tribological performances of the resultant film, J. Phys Chem C., 115 (2011) 10080–10086.
[17] C. Shen, Y. Shen, Y. Wen, H. Wang, W. Liu, Fast and highly efficient removal of dyes under alkaline conditions using magnetic chitosan-Fe(III) hydrogel, Water. Res., 45 (2011) 5200–5210.
[18] T. Feng, S. Xiong, F. Zhang, Application of cross-linked porous chitosan films for Congo red adsorption from aqueous solution, Desal. Water Treat., 53 (2015) 1970–1976.
[19] D.R. Dreyer, S. Park, C.W. Bielawski, R.S. Ruoff, The chemistry of graphene oxide, Chem. Soc. Rev., 39 (2009) 228–240.
[20] D.A. Dikin, S. Stankovich, E.J. Zimney, R.D. Piner, G.H. Dommett, Preparation and characterization of graphene oxide paper, Nature, 448 (2007) 457.
[21] O.C.W. Jr, J.R. Hull, Surface modification of nanophase hydroxyapatite with chitosan, Mater. Sci. Eng: C, 28 (2008) 434–437.
[22] L. Li, L. Fan, C. Luo, H. Duan, X. Wang, Study of fuchsine adsorption on magnetic chitosan/graphene oxide, RSC Adv., 4 (2014) 24679–24685.
[23] P. Sorlier, A. Denuzière, C. Viton, A. Domard, Relation between the degree of acetylation and the electrostatic properties of chitin and chitosan, Biomacro molecules, 2 (2001) 765–772.
[24] H.B. Senturk, D. Ozdes, A. Gundogdu, C. Duran, M. Soylak, Removal of phenol from aqueous solutions by adsorption onto organo modified Tirebolu bentonite: equilibrium, kinetic and thermodynamic study, J. Hazard. Mater., 172 (2009) 353–362.
[25] Y. Sağ, T. Kutsal, Determination of biosorption activation energies of heavy metal ions on Zoogloea ramigera and Rhizopus arrhizus. Process Biochem. Biochem Eng J., 35(2000) 801–807.

[26] T. Fan, Y. Liu, B. Feng, G. Zeng, C. Yang, M. Zhou, H. Zhou, Z. Tan, X. Wang, Biosorption of cadmium(II), zinc(II) and lead(II) by Penicillium simplicissimum: isotherms, kinetics and thermodynamics, J. Hazard. Mater., 160 (2008) 655–661.

[27] Z. Aksu, Equilibrium and kinetic modeling of cadmium(II) biosorption by C. vulgaris in a batch system: effect of temperature, Sep. Purif. Technol., 21 (2001) 285–294.

[28] S.B. R, T.E. Abraham, Biosorption of Cr (VI) from aqueous solution by Rhizopus nigricans, Bioresour Tech., 79 (2001) 73–81.

[29] T. Zhao, T. Feng, Application of modified chitosan micro spheres for nitrate and phosphate adsorption from aqueous solution, RSC Adv., 6 (2016) 90878–90886.

[30] A. Kara, E. Demirbel, N. Tekin, B. Osman, N. Besirli, Magnetic vinyl phenyl boronic acid micro particles for Cr(VI) adsorption: Kinetic, isotherm and thermodynamic studies, J. Hazard. Mater., 286 (2015) 612–623.

[31] Z. Aksu, Biosorption of reactive dyes by dried activated sludge: equilibrium and kinetic modelling, Biochem. Eng J., 7 (2001) 79–84.

[32] T.S. Anirudhan, P.S. Suchithra, Heavy metals uptake from aqueous solutions and industrial wastewaters by humic acid-immobilized polymer/bentonite composite: kinetics and equilibrium modeling, Chem. Eng. J., 156 (2010) 146–156.